

## EXPERIMENTAL STUDY OF THIN PART VIBRATION MODES IN MACHINING

Toufic WEHBE, Gilles DESSEIN, Lionel ARNAUD

**Abstract:** *The machining of thin walls generally generates milling chatter, that damage surface roughness and manufacturing tools. Stability lobes which include natural frequencies are successful in case of tool chatter. When milling thin webs models are less adequate, because the interaction with the tool disrupts the behaviour of the work piece. The modal approach generally used for stability charts may be not adequate enough because of neglecting the tool and the work piece contact. This paper presents the experimental phase of a work aiming at analyse vibration modes of a thin web during machining. A finite element calculation shows the influence of a contact on natural frequencies of the part. For a better investigation, field displacements of the work piece are analysed. This work eventually aims at better knowledge of the contact between the tool and the part to improve the hardness of models.*

**Key words:** *milling, chatter, flexible part, modal shape, displacement field.*

### 1. INTRODUCTION

In milling operations, the machining system is prone to vibratory phenomena that result from the dynamic interaction between the tool and the part. These vibrations called milling chatter generate a poor surface quality, the cutting edge chipping, and the tool and the spindle wear. Many works have been led for more than fifty years in order to study this complex phenomenon. They have shown that chatter control constitutes an industrial and scientific stake.

The source of these vibrations was first identified for turning operation by Tobias [1] and led to the stability lobes theory. Afterwards, this theory was extended to milling [2, 3], and its efficiency was demonstrated for tool vibrations.

However if stability lobes are transposed to flexible work piece, the theory is confronted with a more complex configuration. While vibrating, a thin wall has several modes of vibration, with nodes and antinodes which can be met by the tool. Thus the variable dynamic response of the part according to the tool localization was underlined by [4]. In the same way [5] showed that the contact with the tool as well as the progressive metal removal involve a variation of its dynamic characteristics. A three-dimensional chart of stability lobes including nodes and antinodes makes it possible to see the importance of the position of the tool on the part. Moreover the fast variation of surface quality show behavior changes during the operation, which is specific of thin walls milling. Thus [6] simulates by temporal integration the machining chatter with a moving tool-part contact along the operation. By taking into account the ploughing effect, the mode coupling and the exit of the cut, the model leads to a good correlation with the tests.

Although various works include changes of the part characteristics, stability charts can still contain significant inaccuracy. Indeed the part natural frequencies are measured before the operation in order to

plot stability charts. So the stability lobes theory neglects the tool-part interaction. The disturbance brought to natural modes by the tool presence remains ignored. A better comprehension of this effect requires knowing the real vibratory behavior of the part during its machining.

Experimental works were done to analyze the machining behavior by studying surface qualities, [7] can be quoted. It can be noticed that the complexity is linked to the fact that when a mark of vibration is left by a tooth, the following tooth can erase this information. As a consequence the surface shape which is only a partial trace of the vibratory behavior of the part, does not allow reconstituting the complete history of the operation. To bypass that, we were brought to observe the displacement fields of the part during the operation.

Acoustics also gives only very partial information on machining vibrations [8, 9]. Acceleration measurements usually are utilized [10] but sensors mounting significantly change the structure dynamical properties, according to the added mass proportion. Moreover, displacement obtained by signal integration doesn't give the static deflection of the motion, dependent on the average cutting dynamics. In fact, vibration frequencies obtained by Fast Fourier Transform are mainly utilized for process monitoring. In this application, fixing thresholds on frequencies rather than on measured accelerations is easier and more efficient to detect a change of cutting conditions [11].

As regards chatter control, accelerometer measurements on parts are used especially for the modal analysis before the operation, in order to plot stability lobes. In addition the displacement velocity can be measured by specific Laser velocimetry. This contactless recording has no influence on the operation dynamical behavior. Anyway it can be restricted by lubricant or chips which cross the beam. Velocity measurements were used by [6] and displacement sensors by [7]. Contactless or not measurements are efficient to study specific frequencies values, but do not allow to know the entire work piece

behavior. For such a study, field measurement makes it possible to know the behavior of a structure in any point. This already has been used to identify modal properties of a thin wall [12], but not for machining application.

In order to know real modes of a thin part in machining, a space-time measurement protocol was set up. It is described in the second part. The third part details the machining test procedure. Specific frequencies and real modes shapes analysis are respectively given in fourth part.

## 2. EXPERIMENTAL SETUP

The measurement device illustrated by Fig. 1 was used during machining. On the left side of the part (on the illustration) four accelerometers are fixed in lower part of the tool. Their location will be justified in § 3.2.

On the right side, a Laser vibrometer measures the work piece velocity at its corner, because it is a antinode for all modes shapes. Low frequencies were first removed from the raw signal. Secondly it is integrated to provide the vibratory displacement.

This same side is entirely covered by black and white painting drops. The random resulting gray levels are necessary to measure displacement fields by images stereovision processing. This technique uses images taken at the same instant by the two cameras. The accuracy of stereovision depends on the angle and distance between cameras, sample gray levels, the lighting and an initial calibration phase. Lower accuracy will be reached in case of too weak angle between cameras, too important distance from the work piece, and non homogeneous grey levels or lighting. On top of that noise will be added to results if stereo vision processing parameters are not adapted enough.

Usual applications as tensile tests enable optimized measurement conditions. To measure dynamic phenomena in machining, a specific optimization work has been done. During the machining the two cameras simultaneously take photos at their maximal shooting frequency namely 5.7 Hertz. The cameras are 1 meter far from the work piece. To reduce noise, tests are launched in the dark and the stroboscope is triggered by cameras to visualize the instantaneous deformed part.

All signals are recorded in the same temporal reference mark. Thus accelerations or velocity give the exact starting instant of the machining. The stroboscope signal

Table 1

Eigen frequencies of the instrumented part

	1 <sup>st</sup> mode	2 <sup>nd</sup> mode	3 <sup>rd</sup> mode
Natural frequency (Hz)	520	688	1160
Damping ratio $\xi n$ (%)	1.65	3.6	3.92
Mod. stiffness $Kn$ (N/mm)	132	134	611

and the machining feed speed give the position of the tool for each displacement field.

## 3. MACHINING TESTS PROTOCOL

### 3.1. Validation of the measurement device capacity

Once the device was ready for machining, its capability was evaluated. Beyond a 0.02 mm static displacement perpendicular to the work piece plane, field measurement guarantees an error lower than 5%. For vibration, its capability was validated with a shaker by raising the same modal shapes from accelerations and field measurement [13].

When associated with laser and accelerometer measurements, field measurement is very interesting. In addition to showing the space behavior, it gives the sum of the static and dynamic deformations.

### 3.2. Taking into account the part instrumentation

The machined part is a rectangular aluminum alloy plate (2017 A). It is 50 mm height 2 mm thickness and its clamped length is 110 mm.

The location of the accelerometers was optimized by finite elements calculation to detect the first three modes. They are vertically put at middle height of the part to avoid interference with the tool. The mass of the only plate is 30.7 Grams. It becomes 58.3 grams after instrumentation. This modification was taken into account by hammer test to plot stability lobes (Table 1).

### 3.3. Machining conditions

The operation is a radial down milling. The tool is a cylindrical milling cutter with 4 teeth and 12 mm diameter. Its helix angle is 45°. The feed rate  $f$  is 0.05 mm/tooth and the radial depth of cut is 0.2 mm. The tangential and radial milling force coefficients ( $K_t$  and  $K_r$ ) drawn from the literature [6] are respectively 400 and 40 N/mm<sup>2</sup>. The spindle speed that is worth 24 000 rev/min corresponds at 900 m/min cutting speed.

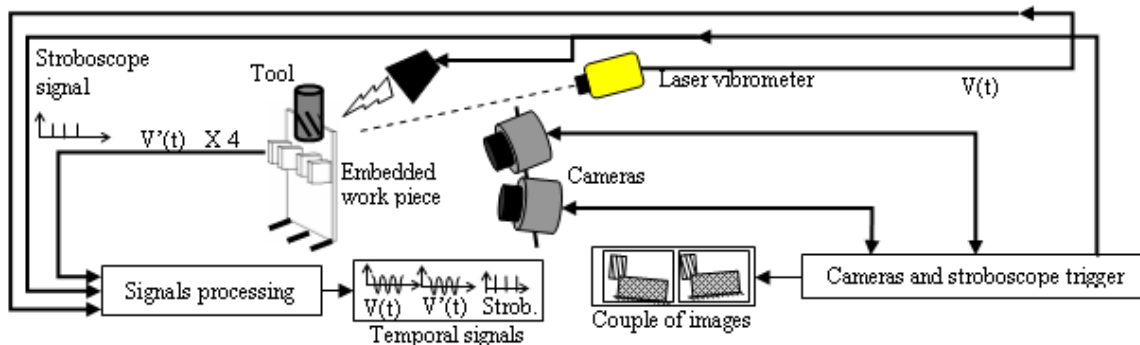


Fig. 1. Measurement set up.

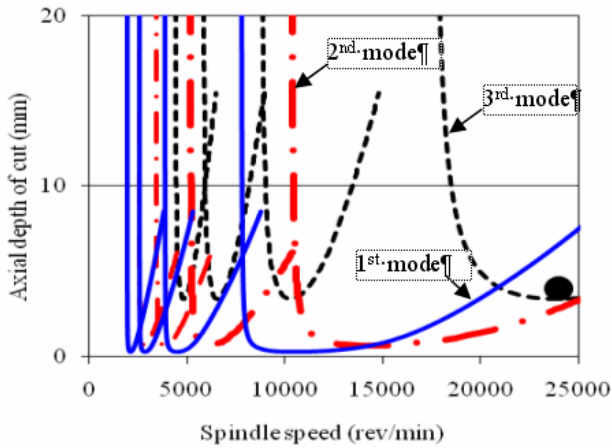


Fig. 2. Layout of the stability chart from [2].

The axial depth of cut  $A_p$  is of 4 mm. On stability lobes according to [2], the test is in unstable zone of lobes of 2<sup>nd</sup> and 3<sup>rd</sup> mode (Fig. 2).

This test takes 1.39 seconds and provides 9 instantaneous field measurements (image gust at 5.7 Hz). In order to statistically obtain images in many configurations (two directions of displacement, crossing at reference position...), the test was repeated 13 times with a different shift of the machining starting departure.

Before each test, part straightness defects are integrated in the tool path in order to guarantee a constant radial engagement. Thereafter this translation of the part is taken into consideration in the analysis. Moreover structural frequencies of each part are systematically measured before the test. This experiment revealed variations going up to 7% on Eigen frequencies, and 57% on damping ratios. These significant variations have many causes: embedding conditions, accelerometers and their cables location errors, and the temperature of the metal.

Plates slightly differ and the plate position related to the angular tool position is not known enough precisely. So conditions of the 1st contact between the tooth and the work piece are not repeatable and tests will not be strictly identical.

#### 4. WORK PIECE SURFACE AND FREQUENCY ANALYSIS

##### 4.1. Analysis of final generated surfaces

The non homogeneous surface quality according to the tool feed reveals the variable part behavior during the machining chronology. In spite of inevitable differences between tests, the most of them shows strong grooves at the beginning. These marks disappear at the center and

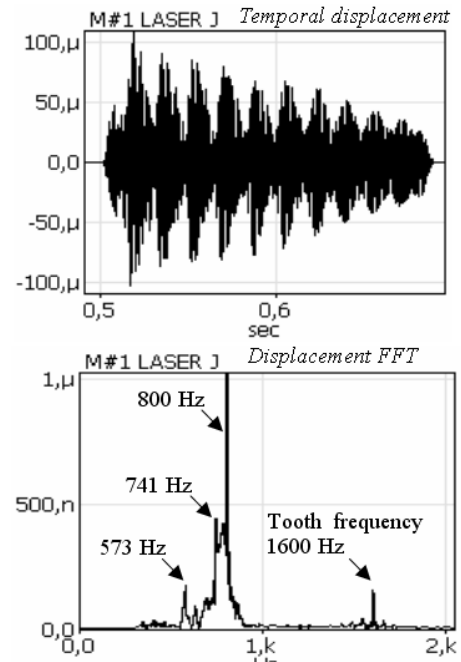


Fig. 4. First zone temporal displacement and frequency.

reappear at exit. At this stage, surface qualities are gathered in three types (Fig. 3) corresponding to similar zones on several parts. In order to validate this procedure and enhance images number, displacements frequencies and amplitudes were compared for the three zones on various parts. This showed a strong agreement and validated the selection of the 3 types.

##### 4.2. Frequency analysis of the three zones

For the first zone which is deeply scratched displacements FFT show four frequencies (Fig. 4).

The two of them being 573 Hz and 1600 Hz have low amplitudes and their impact is not visible on the part. As regards the other frequencies 741 Hz is not far from second mode and 800 Hz exactly corresponds to the half-tooth frequency.

The proximity of these two frequencies induces a global undulation that is visible on temporal signals and on the work piece. This phenomenon frequency is  $(800 - 741 = 59)$  Hz and exactly corresponds to the grooves spacing on the part. Its total amplitude goes from 200  $\mu\text{m}$  to 50  $\mu\text{m}$  but has not been related to grooves height.

The second mode Eigen frequency is worth 688 Hz. Its associated chatter frequency should be close to 850 Hz according to common models. From Flip Lobe models predict it between 700 Hz and 800 Hz. The calculations are not developed here.

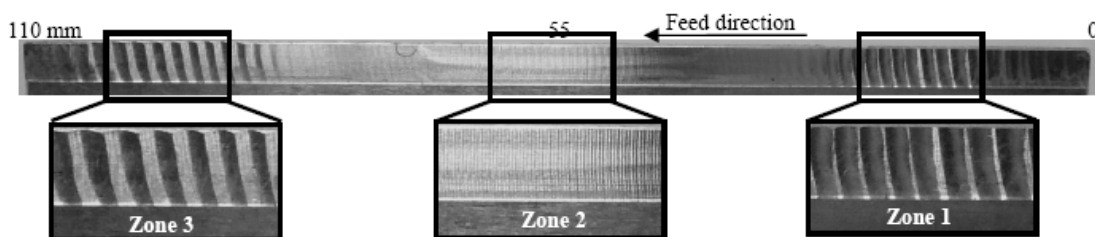


Fig. 3. Selected machining zones.

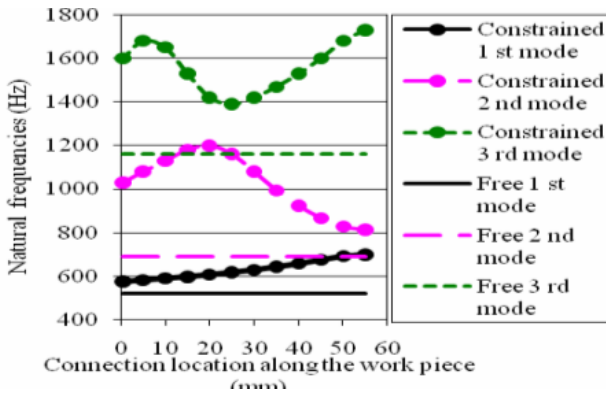


Fig. 5. Natural frequencies variation according to the location of the connection.

For the second zone a better surface quality is shown by Fig. 4. Now dominant frequencies are 3200 Hz (2nd harmonic of tooth crossing frequency), 1600Hz (tooth frequency), 1200 Hz (next to third natural frequency) and 800Hz (half-blow of tooth). Third type looks like the first one by symmetry. The part vibrates at 800 Hz and 758 Hz which are relatively close to the first case. Anyway the scratches of third type are a little bit deeper than those of first one.

4.3. Simplified tool-part contact modeling.

The tool stiffness is worth more than 10 times the parts one, so that it can be considered as undeformable.

By allowing only rotations at the cutting zone, the Eigen frequencies of the part were calculated by finite elements method. This calculation which integrates the metal removal shows that mass loss induces a 5 Hertz variation of the Eigen frequencies. Consequently it is negligible and makes it possible to consider the position of the connection until the medium of the part. Figure 5 gives comparative values of the first three Eigen frequencies with this connection to those of the free part.

This too simplistic modeling does not represent the interaction between the tool tooth and the part enough finely. In the machining the tool and the part are in contact only 50% of time. Nevertheless it is clearly observed that the additional connection significantly increases eigen frequencies. Moreover this effect varies differently according to the connection position and the considered mode. The second structural frequency is highly shifted with the utilized contact.

A less restrictive connection type may bring eigen frequency closer to 741 Hz or 800 Hz. So considering the tool as a constant support on the part seems to be wrong and sophisticated analysis and calculus with other parameters are needed to evaluate that precisely.

4.4. Synthesis of frequencies analysis

Behaviors of the first and third type are similar. In both cases the cutting zone is strongly vibrating. Grooves spacing may be linked to the plate behavior by main vibration periods but not by amplitudes. The recorded vibration frequencies 741 Hz, 758 Hz, 800Hz, 1600Hz and 3200 Hz do not give the contribution of each mode because real modes can't be given by specific recording. The following part details displacement field analysis.

5. SHAPE ANALYSIS DURING MACHINING

5.1. Problematic of instantaneous measured modes

On Fig. 6, the red line called H50 shows the total part displacement next to the tool.

The displacement caused by the only machining is obtained by subtracting the translation H0 of the machine table to correct straightness defects.

When the tool is machining around 20.4 mm from the part edge, several fields show that the deformation has an almost fixed point at 88 mm of the edge. The work piece seems to turn around this point.

As regards the cutting zone it is pushed 125 μm far from the tool and this displacement could correspond to the second modal shape. Anyway the measured node is not central as for the free second mode (symmetrical torsion of the plate), so an overall translation caused by the first mode could be implied. When the tool is at 25.1 mm an additional antinode appears against the tool showing that more complex phenomena can be brought into play.

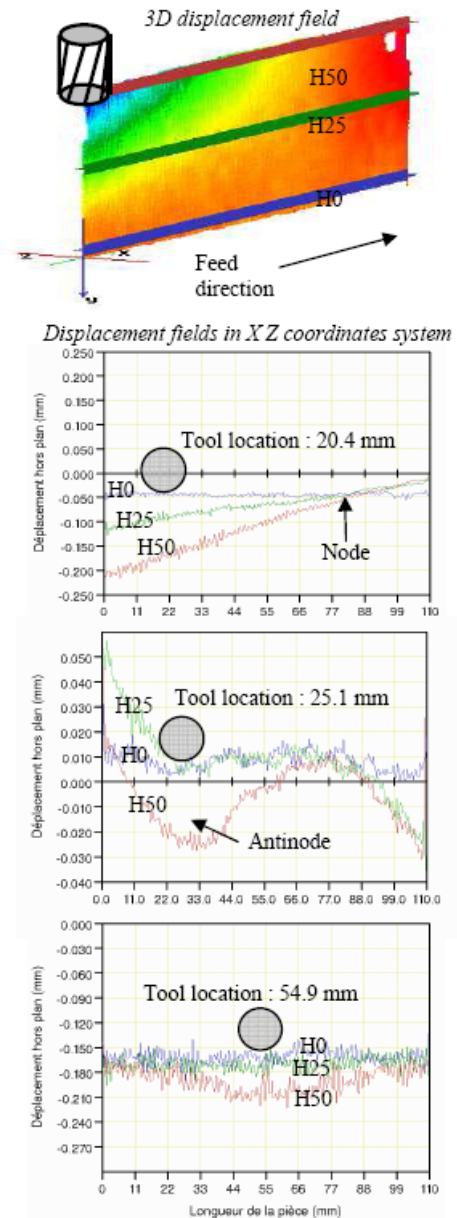


Fig. 6. Displacement fields versus tool position.

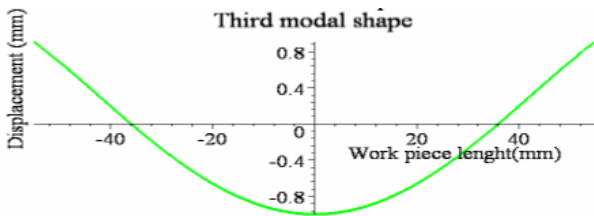


Fig. 7. Polynomials of third modal shape.

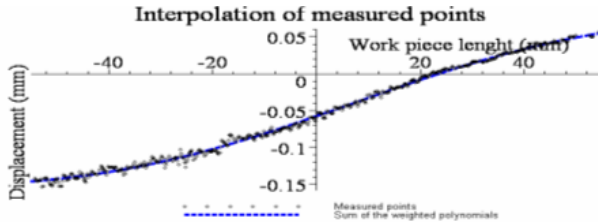


Fig. 8. Interpolation of measurement points.

For the second zone the 40  $\mu\text{m}$  amplitude of the temporal vibrations is hardly linkable to instantaneous displacements when the tool is at 54.9. Indeed in this case the image noise takes an important ratio of weak displacements. Anyway it can be said the part is nearly 30  $\mu\text{m}$  pushed back because of milling dynamics.

At this stage real modes remain impossible to identify visually. That led us to develop a calculus method.

### 5.2. Modes identification method

In order to calculate free modes weights a specific procedure has been built. It aims at finding the weight of each mode so that their sum is superimposed on instantaneous H50 line shape.

First, normalized free modes are calculated by finite elements. Then they are separately interpolated by polynomials with the least square method (see Fig. 7). For 1<sup>st</sup> 2<sup>nd</sup> 3<sup>rd</sup> and 4<sup>th</sup> mode the degrees are respectively 0, 3, 4 and 5.

So each polynomial coefficient takes into account curvatures of the mode in question. Then each polynomial is entirely weighted by a factor (to be determined), that will represent its displacement amplitude contribution.

Secondly for each recording, point coordinates are extracted of the displacement line (H50-H0). The points are then interpolated with least square method by the mode polynomial sum described before (Fig. 8). This step enables to numerically determine modal weights.

### 5.3. Instantaneous free modes recognition

In this test modes higher than third mode don't appear on stability charts. Owing to that only the first four modes are included. Once the identification procedure was applied to the image contributions found are  $-0.051$  for M1,  $0.102$  for M2,  $-0.006$  for M3 and  $-0.003$  for M4. It clearly appears that the second and first modes are dominant on this snap. The third and fourth one have very low amplitudes.

Quote that the snap is instantaneous while the plate is vibrating. At this instant they may be crossing their reference positions and it cannot be concluded that they have no participation. In other words an only one displacement

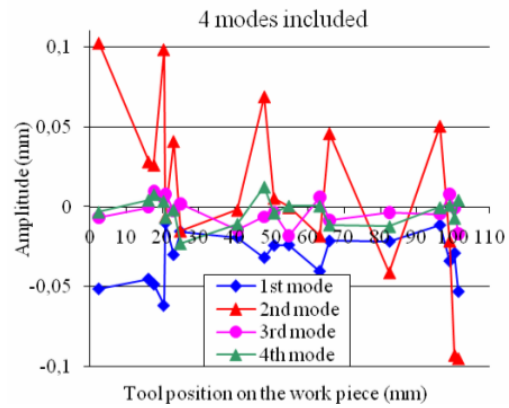


Fig. 9. Modal contributions for the whole operations.

field doesn't let understand the phenomenon during an entire period. Many snaps while milling must be analyzed to know the real behavior.

### 5.4. Modal contribution for the entire milling

Figure 9 displays the modal amplitudes found for the three milling zones of the operation. The second mode amplitude is dominant. The fact that its value can be positive or negative attests a vibratory component of the motion. The amplitude calculated for the first mode is always negative. That shows that the plate seems to vibrate around a static negative value. To verify this hypothesis, static translation induced by milling forces has been investigated. To do that a finite elements calculus led to a 4 Newton cutting force, corresponding to a 33  $\mu\text{m}$  displacement of the cutting zone (averaged value from 13 measurements in 2<sup>nd</sup> zone of the part). The same effort is found with 1<sup>st</sup> and 3<sup>rd</sup> zones, and also correlated by coarse calculus of chip section due to cutting conditions (see § 3.3). Thus for all images the plate deflexion was given by Finite Element method, by applying 4 Newton at the corresponding tool position. The deformed shape was interpolated and then added to modes in the procedure.

Figure 10 displays new modal calculated amplitudes. The second mode amplitude is still dominant. Contrary to the previous results the amplitudes of the first mode oscillate around zero. These more realistic results show the addition of static deflexion to natural modes. In addition interesting information is brought by the envelope of the second mode weights (dark triangles on the graphic). It may be in good agreement to the second modal torsional shape and confirms the higher response of the mode when the tool is exciting its antinodes.

Anyway note that we assumed the milling effort to be constant. That means the feed rate and the radial tooth engagement are also constant. This assumption is still not realistic enough because the measured temporal displacement can reach 100  $\mu\text{m}$  (§ 4.1). Moreover in a minority of cases the modal sum does not superpose on measured points. So the modal calculated weights prove to be not valid for some photos. To be more realistic non constant plate deflexion must be tested. The identification procedure will give solutions but the amplitudes can mathematically be negative. In other words the work piece would be grabbed by the tool. So the identification procedure reaches its limit.

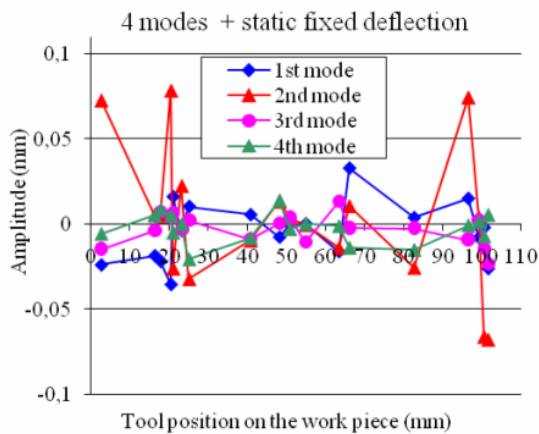


Fig. 10. Modal contributions with static deformation.

### 5.5. Synthesis of shape analysis

The test location on stability lobes suggests the part should mainly vibrate according to its second mode. Nevertheless field analysis showed that first and second free modes and a static deflexion simultaneously appear during machining. The modal identification procedure brings supplementary interesting information. Anyway care must be taken because the first modal shape is much closer to the static deflexion. So to enhance results robustness additional calculus will be done without first mode in the polynomial sum.

## 6. CONCLUSIONS

The analysis of the surface quality and machining behavior led to two reports:

On the one hand measured frequencies are not closed to those predicted by common chatter models which integrate tool free modes. So the tool presence disturbs the natural modes and this effect must be analysed.

On the other hand field measurements show that the real behavior of the part seems result from a static deflection due to the milling forces added to vibration.

As a consequence complementary tests with different cutting conditions must be done to complete this analysis. First they will enable more sophisticated analyses to quantify the contribution of each mode. From that, we will search how the tooth and work-piece interaction disturbs the natural modes. To validate it, the link between modal shapes and frequencies and generated surface will be investigated. Final objectives of this work are to understand the influence of the tool presence on structural modes. It will provide more specific hypothesis to improve current modeling.

## REFERENCES

- [1] Tobias, S.A., Fishwick, W. (1958). *A theory of regenerative chatter*, The Engineer.
- [2] Budak, E., Altintas, Y. (1998). *Analytical prediction of the chatter stability in milling – Part I: General formulation*, Journal of Dynamic Systems, Measurement and Control, Vol. 120, March 1998, pp. 22-30.
- [3] Budak, E., Altintas, Y. (1998). *Analytical prediction of the chatter stability in milling – Part II: Application of the general formulation to common milling systems*, Journal of Dynamic Systems, Measurement and Control, Vol. 120, March 1998, pp. 31-36.
- [4] Lapoujoulade, F., Mabrouki, T., Raïssi, K. (2002). *Prédiction du comportement vibratoire du fraisage latéral de finition des pièces à parois minces (Vibratory behavior prediction of thin-walled parts during lateral finish milling)*, Mécanique et Industrie, Vol. 3, pp. 403-418.
- [5] Thevenot, V., Arnaud, L., Dessein, G., Cazenave Larroche, G. (2006). *Influence of material removal on dynamic behaviour of thin walled structure in peripheral milling*, Machining Science and Technology, Vol.10, p. 275-287.
- [6] Seguy, S., Dessein, G., Arnaud, L. (2008). *Surface roughness variation of thin wall milling, related to modal interactions*, International journal of Machine Tools and Manufacture, Vol.48, September 2007, pp. 261-274.
- [7] Corduan, N., Costes, J.P., Lapoujoulade, F. (2006). *Modeling and experimental approach of milling stability: Application to thin walled parts*, 5<sup>th</sup> International Conference on High Speed Machining, Metz, France.
- [8] Delio, T., Tlustý, J., Smith, S. (1992). *Use of audio signal for chatter detection and control*, Transaction of the ASME, Journal of Engineering for industry, Vol. 114, May 1992, pp. 27-34.
- [9] Prateepasen, A., Au, Y.H.J., Jones, B. (2001). *Acoustic Emission and Vibration for Tool Wear Monitoring in Single-Point Machining Using Belief Network*, IEEE Instrumentation and measurement, May 2001, Technology Conference, Budapest, Hungary.
- [10] Rehorn, A.G., Jiang, J., Orban, P.E. (2005). *State-of-the-art methods and results in tool condition monitoring : a review*, Int J Adv Manuf Technol, Vol. 26, pp. 693-710.
- [11] Orhan, S., Osman, A., Camuscu, N., Aslan, E. (2007). *Tool wear evaluation by vibration analysis during end milling of AISID3 cold work tool steel with 35 HRC hardness*, Independent Nondestructive Testing and Evaluation, Vol. 40, pp. 121-126.
- [12] Girodeau, A., Guo, B. Pierron, F. (2006). *Stiffness and Damping Identification from Full Field Measurements on Vibrating Plates*, Experimental Mechanics, Vol. 46, pp. 777-787.
- [13] Wehbe, T., Seguy, S., Dessein, G., Arnaud, L., Fazzini, M. (2007). *Mesure de champs de déplacements en vibrations : Application à l'usinage de paroi mince (Vibration displacement field measurement of thin web machining)*, August 2007, 18<sup>ème</sup> Congrès Français de Mécanique, Grenoble, France.

## Authors:

Toufic WEHBE, PhD student, Laboratoire Génie de Production, Ecole Nationale d'Ingénieurs de Tarbes, France, E-mail: toufic.wehbe@enit.fr

Gilles DESSEIN, Assistant professor, Laboratoire Génie de Production, Ecole Nationale d'Ingénieurs de Tarbes, France,

E-mail: gilles.dessein@enit.fr

Lionel ARNAUD, Assistant professor, Laboratoire Génie de Production, Ecole Nationale d'Ingénieurs de Tarbes, FRANCE,

E-mail: Lionel.Arnaud@enit.fr